kcal/mol, is probably too low, because MM1 parametrization did not take into account the experimental value of *trans*-methyl-*n*-butyldiazene, which was unavailable at that time. The heats of formation of *trans*-methylethyldiazene and *trans*-diethyldiazene have also been estimated by Rossini et al.[24] to be 28.71 (0.54) and 21.89 (0.92) kcal/mol, respectively, which agree well with the MM2/MOMM values of 29.67 and 23.33 kcal/mol. However, for highly strained molecules, MM2/MOMM results are expected to be more reliable than the group increment method since strains of these molecules are explicitly calculated by the former method.

Isomerization Energies. Calculated isomerization energies for trans–cis geometrical transformations are presented in Table IV. The previous theoretical estimates for the trans–cis isomerization of diimine are in the range of 5.8–7.4 kcal/mol, for which the lower bound is the CEPA value,[13] while the higher bound refers to the STO-3G value. The CEPA value is deemed to be more reliable owing to its handling of electron correlation. The 6-31G//MOMM and 6-31G*//MOMM values are 8.8 and 7.5 kcal/mol, respectively, which are close to the STO-3G value. Similarly, the trans–cis isomerization energies for methyldiazene and azomethane appear to be consistently overestimated by STO-3G, 6-31G//MOMM, and 6-31G*//MOMM. Indeed, Engel et al. have concluded, from studies of thermolysis of cis and trans azoalkanes, that the ground-state energy difference between cis and trans azoalkanes is about 7–8 kcal/mol.[25]

As can be seen in Table IV, MM2/MOMM estimates for trans–cis isomerizations are consistently lower than the corresponding STO-3G, 6-31G//MOMM, and 6-31G*//MOMM values for methyldiazene and azomethane while its estimate reproduces the CEPA value for diimine. The cis–trans isomerization energies for several bridgehead diazenes have recently become known through the important work of Schmittel et al.,[15] and they provide a crucial test for MM2/MOMM parametrizations. The MM2/MOMM values shown in Table IV appear to agree well with all the experimental estimates.[15,25] We calculate the energy difference between *cis*- and *trans*-di-*tert*-butyldiazene to be 24.2 kcal/mol, a value much larger than that in the corresponding alkenes (10.3 kcal/mol). The MM2/MOMM value is also significantly larger than the MM1 value (20.9 kcal/mol). Although the MM1 value is more consistent with the observation[26] that the activation energy for thermolysis of *cis*-di-*tert*-butyldiazene is about 20 kcal/mol less than that of the trans isomer, the recent work of Schmittel[15] appears to favor a value of ca. 25 kcal/mol. Finally, it should be commented that, as far as cis–trans isomerization energy is concerned, MM2/MOMM is more reliable than MM1, since the latter consistently underestimates the steric energy of the cis form.

Conclusions

We have systematically studied the molecular properties of more than 50 azoalkanes. 6-31G//MOMM and 6-31G*//MOMM calculations have been performed to confirm and guide reparametrization. MM2/MOMM parameters are reported for this class of compounds. MM2/MOMM results are generally superior to the previous theoretical results. This work provides an important step for developing a universal, consistent, and unique force field for nitrogen-containing systems.

Acknowledgment. We thank Mr. A. Lilly, Mr. W. Kuhn, Dr. R. Ferguson, and Dr. J. Seeman for their support and comments.

Supplementary Material Available: Experimental and MOMM equilibrium geometries for **1**, **5**, **12**, and **13** (Table II), comparison of theoretical structures for **1–11** (Table III), and predicted $\Delta H_f°$ (Table VI) (7 pages). Ordering information is given on any current masthead page.

(24) Rossini, F. D.; Montgomery, R. L. *J. Chem. Thermodyn.* **1978**, *10*, 465.
(25) Engel, P. S.; Bishop, D. J. *J. Am. Chem. Soc.* **1975**, *97*, 6754.
(26) Mill, T.; Stringham, R. S. *Tetrahedron Lett.* **1969**, 1853.

Empirical Potential Energy Surfaces Relating Structure and Activation Energy. 2. Determination of Transition-State Structure for the Spontaneous Hydrolysis of Axial Tetrahydropyranyl Acetals

Hans-Beat Bürgi* and Katharina C. Dubler-Steudle

Contribution from the Laboratory for Chemical and Mineralogical Crystallography, University of Berne, CH-3012 Berne, Switzerland. *Received December 31, 1987*

Abstract: Experimental ground-state structural data and valence force constants are combined with activation energy estimates to obtain energy surfaces describing bond-breaking reactions. The model may be used to describe systematic variations in the structural and energetic behavior of families of related molecules undergoing the same type of reaction and provides estimates of transition-state structure. For spontaneous acetal hydrolysis, which is discussed as an example, changes in ground-state structure are related to changes in free energy of activation in a quantitative way, and the calculated transition-state structures are shown to be compatible with available experimental and theoretical evidence on related systems.

Recently, we have developed models relating free energy of activation with ground-state structure for series of related molecules undergoing the same type of reaction.[1,2] The basic idea is to parametrize a simplified potential energy surface with the help of structural, vibrational, and kinetic data pertaining to an arbitrarily chosen reference molecule and its reaction intermediate. Energy surfaces for the remaining molecules in the series are obtained by applying a simple perturbation to the reference surface. As a test of the model, perturbed ground-state structure and free energy of activation are calculated and compared to experimental quantities. This procedure provides insight into a sometimes dramatic dependence of reaction rate on small struc-

(1) Bürgi, H.-B.; Dunitz, J. D. *J. Am. Chem. Soc.* **1987**, *109*, 2924–2926.
(2) Bürgi, H.-B.; Dubler-Steudle, K. C. *J. Am. Chem. Soc.* **1988**, *110*, 4953–4957.

0002-7863/88/1510-7291$01.50/0

Chart I[a]

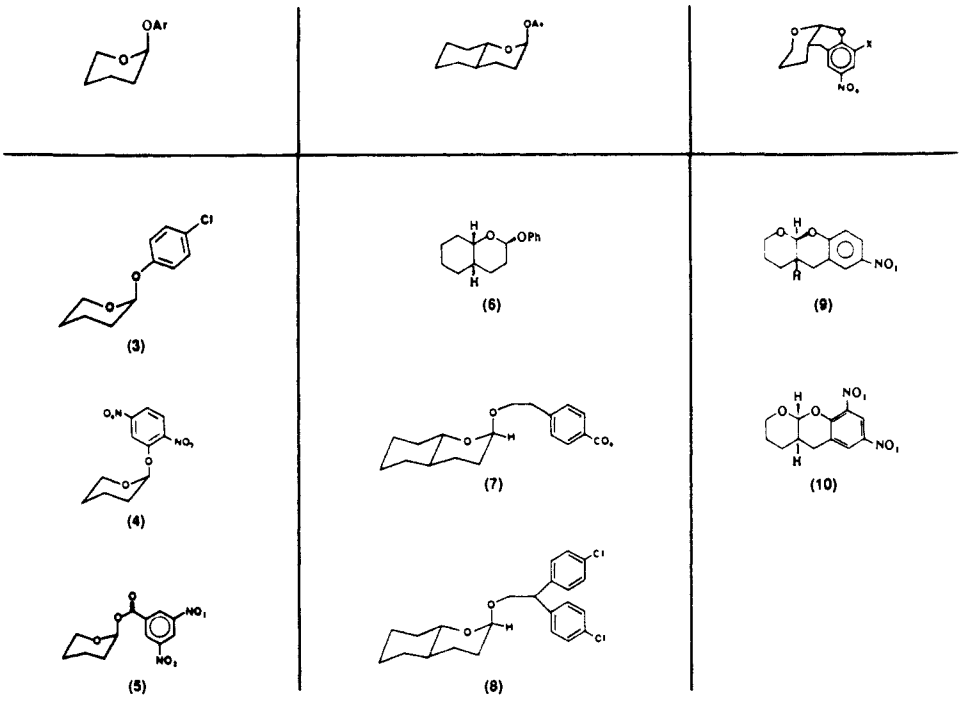

[a] Key: **3**, 2-(4-chlorophenoxy)tetrahydropyran; **4**, 2-(2,5-dinitrophenoxy)tetrahydropyran; **5**, 2-[(3,5-dinitrobenzoyl)oxy]tetrahydropyran cyclohexane solvate; **6**, 2a-phenoxy-*trans*-1-oxadecalin; **7**, 2α-[2-(4-carboxyphenyl)ethoxy]-*trans*-1-oxadecalin; **8**, 2α-[2,2-bis(4-chlorophenyl)ethoxy]-*trans*-1-oxadecalin; **9**, 3,4,4aα,10aα-tetrahydro-7-nitro-2*H*,5*H*-[1]benzopyrano[2,3-*b*]pyran; **10**, 3,4,4aα,10aα-tetrahydro-7,9-dinitro-2*H*,5*H*-[1]-benzopyran[2,3-*b*]pyran.

tural differences in the ground state. As a byproduct, estimates of transition-state structure are obtained.

The determination of transition-state structure is a long-standing problem. Modern ab initio methods can sometimes provide a solution for reactions in the gas phase. Structural information on transition states in solution is usually derived indirectly from mechanistic interpretations of kinetic data. Although such information is abundant, it is almost always relative to some reference structure, e.g. the structure of a reactant, intermediate, or product. Correspondingly, the language to describe transition-state structure uses terms such as "reactant-like", "product-like", or "intermediate-like". Similarly, related transition states for similar substrates undergoing the same type of reaction are usually classified as "earlier" or "later", "looser" or "tighter" than some reference, which itself is not known on an absolute scale.[3] The approach to be described in this paper aims at a determination of absolute transition-state structure for solution reactions. It is based on an understanding of the relationship between small changes of molecular structure in the ground state and associated changes in reaction rate.

The case of spontaneous hydrolysis of aryl tetrahydropyranyl acetals (**1**) is discussed as an example[4,5] (Chart I). The generally

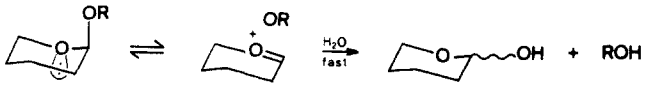

(1) (2)

accepted mechanism is a unimolecular decomposition to a phenoxide anion and an oxocarbenium cation (**2**), the C–OR cleavage being the rate-determining step. Jones and Kirby[4-6] have shown that the reaction is subject to stereoelectronic control. The heterolytic cleavage occurs readily only if a lone pair of the ring

Chart II

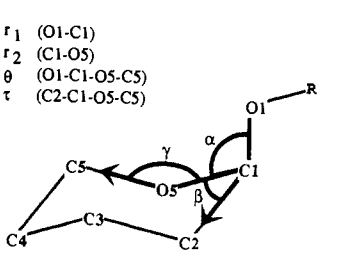

oxygen atom is antiperiplanar to the bond being broken (**1**). In contrast, the equatorial isomers are stable if their conformation is fixed. The detailed structure and the rate of hydrolysis of **1** depends on R: the larger its electron-withdrawing power, the lower the energy of the antibonding σ*(C–OAr) orbital and the larger the anomeric interaction with the axial orbital of the lone pair on the ring oxygen. A corresponding shortening of the endocyclic C–O bond and a lengthening of the bond to the leaving group are observed for the reactant. Within the observable range, both C–O bond lengths show an approximately linear dependence on the pK_a of the conjugate acid of the leaving group, ArOH. Likewise, the logarithm of the rate constant for the hydrolysis of these compounds, log k_{hyd}, is a linear function of the pK_a of ArOH.[7] Extrapolation of the linear relationship between the lengthening of the exocyclic C–OR bond and the activation energy for heterolytic cleavage led Jones and Kirby[6,7] to an estimate of 1.56 Å for the exocyclic C–OR bond length in the transition state, in sharp disagreement to their statement that the reaction should proceed via a late transition state, close in structure to the ionic intermediates.

If the model sketched above is applied to spontaneous acetal hydrolysis, a correlation between reactant structure and activation energy is obtained that agrees with the experimental data given by Jones and Kirby.[4,5] The calculated transition-state structures are shown to be late, thus resolving the contradiction in the earlier work.[6,7]

(3) Several review articles are found in: *Transition States of Biochemical Processes*; Gandour, R. D., Schowen, R. L., Eds.; Plenum: New York, 1978.
(4) Jones, P. G.; Kirby, A. J. *J. Chem. Soc., Chem. Commun.* **1979**, 288–289.
(5) Briggs, A. J.; Glenn, R.; Jones, P. G.; Kirby, A. J.; Ramaswamy, P. *J. Am. Chem. Soc.* **1984**, *106*, 6200–6206.
(6) Jones, P. G.; Kirby, A. J. *J. Am. Chem. Soc.* **1984**, *106*, 6207–6212.
(7) Craze, G.-A.; Kirby, A. J. *J. Chem. Soc., Perkin Trans. 2* **1978**, 354–356.

Table I. Selected Structural Parameters of Eight Axial Tetrahydropyranyl Acetals[a]

compd	ref	R–O1	O1–C1 (r_1)	C1–C2	C2–C3	C3–C4	C4–C5	C5–O5	C1–O5 (r_2)
3	8	1.369	1.427	1.502	1.506	1.513	1.505	1.430	1.398
4	9	1.354	1.458	1.501	1.516	1.504	1.509	1.445	1.383
5	10	1.328	1.476	1.482	1.465	1.468	1.464	1.414	1.379
6	11	1.378	1.433	1.505	1.532	1.520	1.520	1.448	1.405
7	12	1.404	1.411	1.504	1.519	1.527	1.506	1.434	1.428
8	12	1.423	1.406	1.491	1.519	1.523	1.502	1.441	1.416
9	13	1.364	1.448	1.515	1.532	1.522	1.507	1.436	1.385
10	14	1.351	1.466	1.516	1.517	1.526	1.509	1.433	1.377

compd	R–O1–C1	O1–C1–C2	O1–C1–O5 (α)	C2–C1–O5 (β)	C1–C2–C3	C1–O5–C5 (γ)
3	119.6	106.1	111.7	112.7	111.8	113.7
4	118.8	105.3	110.1	114.8	111.4	113.8
5	117.1	108.8	106.6	114.0	112.4	113.8
6	118.9	106.4	111.6	113.1	111.4	114.0
7	115.8	108.4	110.2	112.8	111.3	113.9
8	114.8	108.7	111.4	112.7	111.4	113.8
9	119.6	111.8	105.9	113.6	110.7	114.1
10	118.6	110.8	105.4	114.5	110.4	114.9

compd	R–O1–C1–O5	O1–C1–C2–C3	O1–C1–O5–C5 (θ)	C1–O5–C5–C4	C2–C1–O5–C5 (τ)
3	64.3	−69.2	64.3	56.5	−55.1
4	55.1	−70.9	66.2	55.1	−52.3
5	110.8	−72.8	69.9	57.3	−50.2
6	66.9	−70.8	64.6	57.3	−55.3
7	65.7	−72.0	67.3	59.3	−54.0
8	64.6	−72.4	67.1	58.3	−55.3
9	−158.1	−67.4	67.5	57.0	−55.5
10	−164.0	−67.9	69.2	55.0	−52.8

[a] Bond lengths are in angstroms, and angles are in degrees.

Table II. Results of Principal-Component Analysis on Covariance Matrix of Five Structural Parameters

	distances, Å		angles, deg
	Means and Standard Deviations		
r_1	1.441 (0.026)		
r_2	1.396 (0.019)		
β_s	2.881 (0.021)	β	113.5 (8)
γ_s	2.822 (0.010)	γ	114.0 (4)
θ_s	1.659 (0.049)	θ	67.0 (2.0)

	PRIN1	PRIN2	PRIN3
eigenvalues, Å^2	0.002925	0.000812	0.000090
fraction of total variance	0.748	0.208	0.023
eigenvectors, Å			
r_1	0.356	0.566	−0.379
r_2	−0.217	−0.478	0.312
β_s	0.262	0.453	0.725
γ_s	0.089	0.036	0.481
θ_s	0.866	−0.494	−0.035

Experimental Part

Data Retrieval and Processing. Crystal structures of eight axial acetals[8-14] (Chart I) are available from the literature (**3–10**). The fragment shown in Chart II is present in each compound. The observed values of 19 structural parameters of this fragment are listed in Table I. Statistical analyses were performed on a reduced data set, limited to variables relevant to acetal cleavage. This helps to avoid bias in the results due to various systematic deficiencies of the data. For example, variances of certain angles are large because of differences in constitution (e.g. R–O1–C1–O5, R–O1–C1, O1–C1–O5, and O1–C1–C2; Table I and Chart I); for compound **5**[10] temperature factors of the tetrahydropyranyl

Chart III

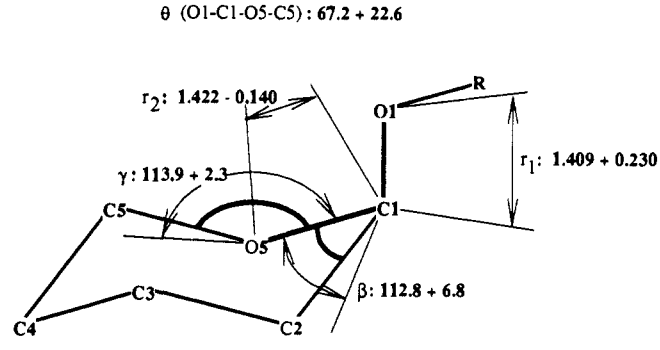

Bond lengths in Å, angles in deg.

carbon atoms are high and the corresponding bond lengths are therefore systematically too short (Table I; presence of a disordered cyclohexane molecule). Parameters pertaining to hydrogen atoms are excluded altogether because the values determined by X-ray diffraction are generally of low accuracy. The reduced fragment consists of the three atoms O1, C1, and O5 and the bond vectors to C2 and C5 (Chart II). Its geometry is described by seven internal coordinates, chosen as the exocyclic bond length O1–C1 (r_1), the endocyclic bond length C1–O5 (r_2), the three angles O1–C1–O5 (α), C2–C1–O5 (β), and C1–O5–C5 (γ), and the torsion angles O1–C1–O5–C5 (θ) and C2–C1–O5–C5 (τ). The mean value of the two bond lengths O1–C1 and C1–O5 from all eight acetals compounds, 1.4185 Å, was used for scaling angles to length units; e.g. $\alpha_s = 1.4185\pi\alpha/180°$ Å, etc. The scaled parameters, used in subsequent analyses, are listed in Table I of the supplementary material.

Principal component analyses[15] were done with the program SAS[16] on

(8) Jones, P. G.; Sheldrick, G. M.; Kirby, A. J.; Glenn, R.; Ramaswamy, P.; Halstenberg, M. *Z. Kristallogr.* **1982**, *159*, 265–270.
(9) Jones, P. G.; Sheldrick, G. M.; Kirby, A. J.; Glenn, R. *Z. Kristallogr.* **1982**, *161*, 253–258.
(10) Jones, P. G.; Sheldrick, G. M.; Glenn, R.; Kirby, A. J.; Ramaswamy, P. *Z. Kristallogr.* **1983**, *163*, 93–100.
(11) Jones, P. G.; Kennard, O.; Chandrasekhar, S.; Kirby, A. J. *Acta Crystallogr., Sect. B: Struct. Crystallogr. Cryst. Chem.* **1978**, *B34*, 2947–2949.
(12) Jones, P. G.; Sheldrick, G. M.; Kirby, A. J.; Briggs, A. J. *Acta Crystallogr., Sect. C: Cryst. Struct. Commun.* **1985**, *C41*, 1380–1383.
(13) Jones, P. G.; Kennard, O.; Kirby, A. J.; Martin, R. J. *Acta Crystallogr., Sect. B: Struct. Crystallogr. Cryst. Chem.* **1979**, *B35*, 242–244.
(14) Jones, P. G.; Kennard, O.; Kirby, A. J.; Martin, R. J. *Acta Crystallogr., Sect. B: Struct. Crystallogr. Cryst. Chem.* **1979**, *B35*, 755–757.

(15) Factor analysis is a method to analyze covariance (correlation) of multivariate systems. The covariance (correlation) matrix is transformed to an eigenvector basis ranked according to eigenvalues. Very often some of the smaller eigenvalues account for an insignificant fraction of the total variance (correlation) and the corresponding eigenvectors are dropped. The total number of variables is thus reduced to a smaller number of significant factors, which should account for most of the variance (correlation). For a general reference, see: Malinowski, E. R.; Howery, D. G. *Factor Analysis in Chemistry*; Wiley-Interscience: New York, 1980. For applications in structural chemistry, see: (a) Murray-Rust, P.; Motherwell, S. *Acta Crystallogr., Sect. B: Struct. Crystallogr. Cryst. Chem.* **1978**, *B34*, 2518–2526. (b) Murray-Rust, P. *Acta Crystallogr., Sect. B: Struct. Crystallogr. Cryst. Chem.* **1982**, *B38*, 2765–2771.

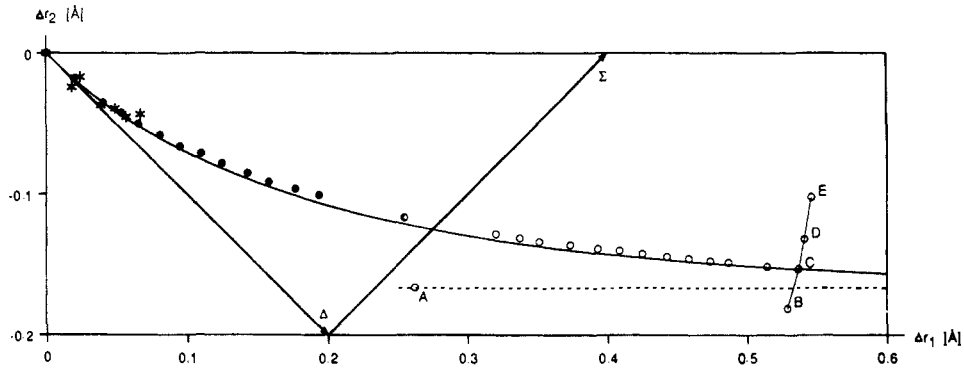

Figure 1. $\Delta r_1 = r_1 - r_{10}$ versus $\Delta r_2 = r_2 - r_{20}$ (a) along a line of constant bond order (solid curve), (b) as extrapolated from factor analysis (point A), (c) for several transition-state structures with energy $E_0^{\ddagger}$ (points B–E), (d) for perturbed ground- and transition-state structures (filled and empty circles, respectively; the points are to be taken in pairs, the point at the origin with point C, etc.; ground- and transition-state structures coincide for the half-filled circle); the dotted line indicates the estimated value of Δr_2 in the reaction intermediate **2**. For arrows labeled Σ and Δ see footnote 29.

both correlation and covariance matrices including **5** (r_1, r_2, β, γ, θ), **6** (r_1, r_2, β, γ, θ, τ), and **7** (r_1, r_2, α, β, γ, θ, τ) parameters, respectively.

Results and Discussion

Principal Component Analysis[15] of (Scaled) Internal Coordinates. The most important results of a typical covariance analysis are listed in Table II. The first two principal components contain 95.6% of the total variance. With an eigenvalue of 0.0029 Å^2, the first component, PRIN1, accounts for 74.8% and the second, PRIN2, for 20.8% (0.0008 Å^2). The third principal component, with an eigenvalue of 0.00009 Å^2 (2.3%), is comparable in magnitude with the average experimental variances: 0.00003 Å^2 for bond distances and 0.00008 Å^2 for angles (scaled); it is considered chemically irrelevant. The five-dimensional problem is thus reduced to a two-dimensional one. The eigenvector of PRIN1 indicates that, as the exocyclic bond O1–C1 (r_1) lengthens, the endocyclic bond C1–O5 (r_2) shortens, the bond angle at O5 (γ) increases slightly, the one at C1 (β) increases much more strongly, and the torsion angle θ increases. All of these changes and the correlation between them are easily interpreted in terms of incipient hydrolysis of the acetal fragment, as already noted by Jones and Kirby.[4-6] A qualitative graphical representation of these movements may be found in Chart III (the numbers are explained in the next section). There is no obvious chemical interpretation for the second eigenvector (PRIN2); it shows approximately the same correlation between r_1, r_2, β, and γ as PRIN1 but opposite sign for the component in θ. We take the point of view that the angle θ is affected not only by the nature of the exocyclic acetal substituent but also by the different kinds of ring systems (Chart I). The contribution of θ to the first two principal components may well be different for a different sample of structures. This part of the eigenvector should be taken with a grain of salt.

From a corresponding analysis of the correlation matrix, the first two eigenvalues are found to be 3.36 and 0.84. The first eigenvector is (+0.52, −0.49, +0.50, +0.33, +0.36); i.e., the results are very similar to those obtained from the covariance matrix.

If more variables are analyzed, results remain practically the same; especially, the contribution of r_1, r_2, β, and γ to the first eigenvector is quite similar for **5**–**7** variables from both covariance and correlation matrices. This eigenvector is thus a robust feature of the analysis.

Extrapolation toward a Transition-State Structure. To the extent that the eigenvector belonging to the first principal component describes incipient acetal cleavage, it might serve as a pointer in the general direction of the transition-state structure. A simple-minded estimate of such a structure may be obtained by linear extrapolation along this vector (toward point A in Figure 1). Immediately, the question arises as to how far to go. For a late transition state,[2-5] the (−C1=O5$^+$−) distance can be estimated to be about 1.28 Å, somewhat larger than those found in analogues of the reaction intermediate **2**, e.g. the 2-norbornyl cation, 2-methoxy-1,7,7-trimethylbicyclo[2.2.1]hept-2-ylium fluoroborate (1.256 (5) Å, **11**)[17] and the cations HO=CH$_2^+$

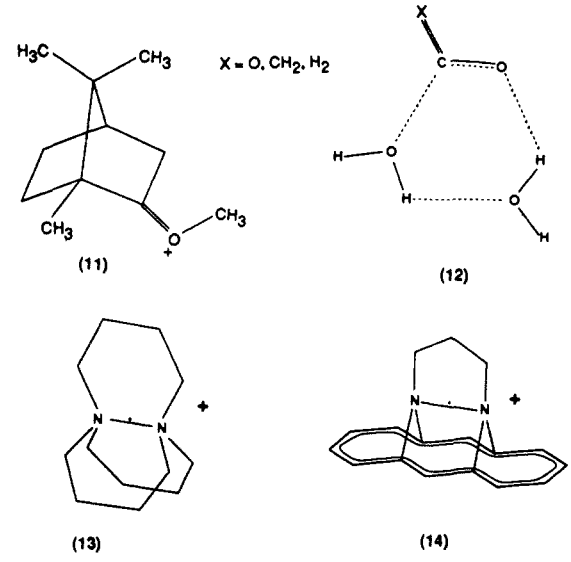

(1.246 Å)[18] and CH$_3$O=CH$_2^+$ (1.234 Å).[19] With this constraint the transition-state structure is located 0.645 unit vectors from the mean structure in the direction of PRIN1. Chart III shows reference structural parameters obtained by averaging the data for compounds **7** and **8** and the changes of these parameters necessary to reach the transition-state structure. The distances and angles derived in this way for the transition state seem reasonable. The angle $\beta^{\ddagger}$ (C2–C1–O5) is about 120° (as expected for an sp^2-hybridized carbon). The angle $\gamma^{\ddagger}$ (C1–O5–C2) is about 116°, slightly less than 120° (sp^2-hybridized oxygen with one lone pair); the torsion angle $\theta^{\ddagger}$ of 80–90° puts the leaving group O1 into the nodal plane of the p_π orbitals on C1 and O5 as already pointed out by Jones and Kirby.[5,6] γ decreases to $\gamma^{\ddagger} \approx 30°$, indicating a flattening of the six-membered ring. The angle $\alpha^{\ddagger} \approx 80$–90° is too small compared with earlier results on the angle of nucleophilic attack at carbonyl groups (100–110°);[20] this may reflect a particularly severe influence of the differences in constitution on α (Chart I). The extrapolated estimate of $r_1^{\ddagger}$ (O1–C1) is 1.66 Å, 0.10 Å longer than that given by Jones and Kirby but still relatively short for a late transition state. This estimate may

(16) *SAS User's Guide: Statistics Version 5 Edition*; SAS Institute: Cary, NC, 1985.

(17) Montgomery, L. K.; Grendze, M. P.; Huffman, J. C. *J. Am. Chem. Soc.* **1987**, *109*, 4749–4750.

(18) Nobes, R. H.; Radom, L.; Rodwell, W. R. *Chem. Phys. Lett.* **1980**, *74*, 269–272 (basis set 4-31G).

(19) Nobes, R. H.; Rodwell, W. R.; Bouma, W. J.; Radom, L. *J. Am. Chem. Soc.* **1981**, *103*, 1913–1922 (basis set 4-31G).

(20) Bürgi, H. B.; Dunitz, J. D.; Shefter, E. *J. Am. Chem. Soc.* **1973**, *95*, 5065–5067.

be taken as a lower limit to $r_1^{\ddagger}$, since linear extrapolation can hardly be expected to hold for large changes in bond distances. As described elsewhere[21,22] and as noted by Jones and Kirby,[6] the simultaneous change of two bond distances, e.g. two acetal C–O bond lengths, follows the rule of conservation of bond order n: n_1 (O1–C1) + n_2 (C1–O5) ≈ constant. With Pauling's bond order–bond distance relationship,[23] $r_1 = r_{10} - c \log n_1$, $r_2 = r_{20} - c \log n_2$, the dependence of r_1 on r_2 is hyperboloid (Figure 1, solid curve). At r_2 (C1–O5) = 1.28 Å, r_1 (O1–C1) is about 1.8 Å. As the distance r_2 (C1–O5) approaches 1.25 Å asymptotically, r_1 (O1–C1) tends to infinity. A chemically meaningful upper limit to $r_1^{\ddagger}$ may be taken as the C···O van der Waals distance of 3 Å.

In summary, the analysis of structural parameters indicates a transition-state structure with $r_1^{\ddagger}$ (O1–C1) in the range 1.6–3 Å, $r_2^{\ddagger}$ (C1–O5) close to 1.25 Å and a planar conformation of the CH_2—O^+=C—CH_2 fragment with angles of 116 and 120° at O^+ and C, respectively.

Correlations between Activation Energies and C–O Bond Lengths. In this paragraph structure and energy are considered together with the aim of narrowing the range of possible transition-state structures. The general idea is as follows: given a series of related molecules undergoing a similar reaction, the change in energy along the reaction profile for one of these molecules (the reference molecule) is associated with a particular functional form. Corresponding energy functions for the other molecules are then obtained by applying a perturbation on the reference energy surface. The perturbed fragments will show changes in free energies of activation, in equilibrium- and transition-state structures. From these changes the change of activation energy with change in ground-state structure may be calculated and compared to experiment.

For subsequent analysis the reference C–O distances are chosen as r_{10} = 1.422 Å and r_{20} = 1.409 Å. These numbers are averages from molecules **7** and **8**, which have the poorest leaving groups, the smallest r_1, and the largest r_2. The constant c in Pauling's equation is found to be 0.24 Å from **7**, **8**, and **11**. The reference free energy of activation $E_0^{\ddagger}$ is 38.85 kcal mol^{-1} (from **7** and **8**).[4]

Reaction Profile, One-Dimensional Model. Various functions may be chosen to represent the dependence of energy E on the reaction coordinate q, e.g. a Morse potential, with exponential[22] (n) or linear[24] perturbation (a):

$$E(q) = E_0^{\ddagger}[\exp(-2bq) - 2n \exp(-bq)] \qquad 0 \le n \le 1$$

$$E(q) = E_0^{\ddagger}[\exp(-2bq) - 2 \exp(-bq) + aq] \qquad a \le 0$$

Alternatively a simple cubic polynomial with linear perturbation (a) may be used.[25]

$$E(q) = -E_0^{\ddagger} + (k_q q^2/2 + k_{qq} q^3 + aq) \qquad a \le 0$$

Here, k_q is the quadratic force constant along q, and k_{qq} is the corresponding anharmonicity constant. The unperturbed functions depend on two parameters: $E_0^{\ddagger}$ and k_q[26] (for the Morse function $k_q = 2b^2E_0^{\ddagger}$).[2]

$E_0^{\ddagger}$ is taken as the experimental free energy of activation of the reference molecule; k_q is obtained from ab initio calculation (5.07 mdyn Å^{-1}; see the section on two-dimensional models, below). Activation energies $E^{\ddagger}$, ground-state equilibrium coordinates q_E, and transition-state coordinates q_{TS} are then calculated for increasing perturbations. The dependence of $E^{\ddagger}$ on q_E is $E^{\ddagger} = E_0^{\ddagger}[1 - 2q_E(k_q/6E_0^{\ddagger})^{1/2}]^3$; it is plotted in Figure 2 and compared with the experimental results for which q_E(obs) is taken as $[(r_1 - 1.422)^2 + (r_2 - 1.409)^2]^{1/2}$ [Å]. It is seen that the cubic potential energy function accounts best for the experiments (Figure 2, solid line). Thus, the observed change in ratios $E^{\ddagger}/E_0^{\ddagger}$ is modeled quite well by a *single independent* parameter, namely the force constant k_q. Figure 3 shows corresponding potential functions for the reference molecule and a perturbed molecule; the transition state for the reference molecule is at $q_{TS} \approx 0.56$ Å. If we require this point to be on the line of constant bond order (Figure 1, solid curve), we obtain $r_1^{\ddagger} \approx 1.409 + 0.54 \approx 1.96$ Å and $r_2^{\ddagger} \approx 1.422 - 0.15 \approx 1.27$ Å, well within the range deduced from structural parameters alone. For a perturbed molecule q_E increases, q_{TS} decreases by the same amount, and $E^{\ddagger}$ decreases, in agreement with Hammond's postulate.[27] The observed range of q_E is 0.08 Å, that of q_{TS} is the same. The value of k_{qq}[26] is −2.99 mdyn Å^{-2}, corresponding to an anharmonicity constant $b = -2k_{qq}/k_q \approx 1.18$ Å^{-1}. This is the right order of magnitude if compared to spectroscopic values of 1.5–2.5 Å^{-1}.[28]

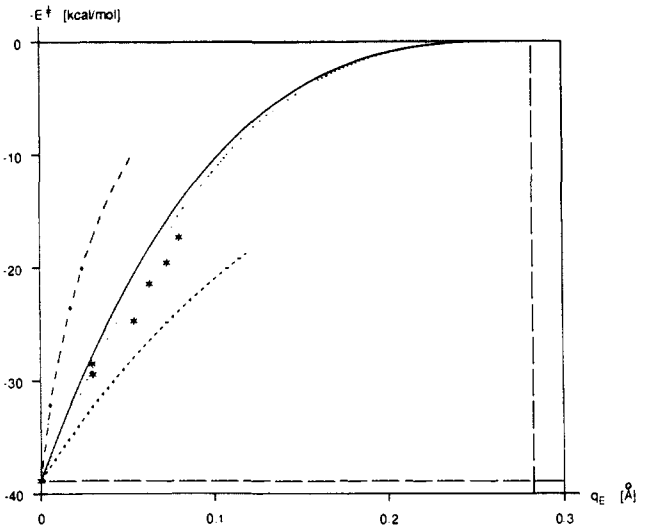

Figure 2. Dependence of activation energy ($E^{\ddagger}$) on ground-state equilibrium structure (q_E) for various models $E(q)$: solid line, cubic polynomial in q; dotted line, cubic polynomial in Δr_1 and Δr_2; dot–dashed line, Morse function with linear perturbation; dashed line, Morse function with exponential perturbation; stars, experimental quantities.

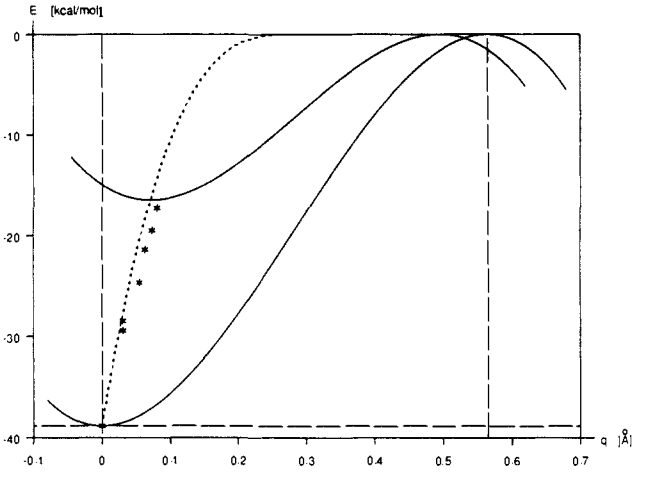

Figure 3. Comparison of structure–reactivity correlation, $E^{\ddagger}$ versus q_E (dashed line), with reaction profiles $E(q)$ for an unperturbed and a perturbed molecule (solid lines).

Reaction Profile, Two-Dimensional Model. Since acetal cleavage involves significant changes in at least two bond distances,

(21) Bürgi, H.-B. *Angew. Chem.* **1975**, *87*, 461–475; *Angew. Chem., Int. Ed. Engl.* **1975**, *14*, 460–473.
(22) Dunitz, J. D. *X-ray Analysis and the Structure of Organic Molecules*; Cornell University: Ithaca, NY, 1979.
(23) Pauling, L. *The Nature of the Chemical Bond*; Cornell University: Ithaca, NY, 1960.
(24) Bersuker, I. B. *Teor. Eksp. Khim.* **1978**, *14*, 3.
(25) Bersuker, I. B. *The Jahn–Teller Effect and Vibronic Interactions in Modern Chemistry*; Plenum: New York, 1984.
(26) When $dE/dq = 0$ is used, it may be shown that $k_{qq} = -k_q/(3q_{TS})$, where q_{TS} is the distance along q between ground and transition state. For the Morse function the relationship $k_q = 2b^2E_0^{\ddagger}$ holds.[2]
(27) Hammond, G. S. *J. Am. Chem. Soc.* **1955**, *77*, 334–338.
(28) For a compilation, see: Mills, I. M. *Theor. Chem. (London)* **1974**, *1*, 110–159.

Table III. Numerical Constants Characterizing the Energy Surface $E = k_{11}(\Delta r_1^2 + \Delta r_2^2)/2 + k_{12}\Delta r_1\Delta r_2 + k_{111}(\Delta r_1^3 + \Delta r_2^3) + k_{112}(\Delta r_1^2\Delta r_2 + \Delta r_1\Delta r_2^2)$ and Calculated Transition-State Properties (for References See Text)

	Ground State		
r_{10}	1.422 Å	k_{12}/k_{11}	0.05
r_{20}	1.409 Å	$k_{111} = k_{222}$	-2.18 mdyn Å^{-2}
$k_{11} = k_{22}$	5.34 mdyn Å^{-1}	$k_{112} = k_{122}$	6.70 mdyn Å^{-2}
	Transition State		
r_1^*	1.95 Å	k_{12}^*	-9.1 mdyn Å^{-1}
r_2^*	1.27 Å	k_{22}^*	10.8 mdyn Å^{-1}
k_{11}^*	0 mdyn Å^{-1}	E_0^*	38.85 kcal mol^{-1}

a more complete model energy surface should take both of them into account. In analogy to the one-dimensional model, we chose

$$E = k_{11}(\Delta r_1^2 + \Delta r_2^2)/2 + k_{12}\Delta r_1\Delta r_2 + k_{111}(\Delta r_1^3 + \Delta r_2^3) + k_{112}(\Delta r_1^2\Delta r_2 + \Delta r_1\Delta r_2^2)$$

i.e. a cubic polynomial in $\Delta r_1 = r_1 - r_{10}$ and $\Delta r_2 = r_2 - r_{20}$ where we include the constraint that the two bonds r_1 and r_2 are assumed to be equivalent.[29]

The analysis will proceed in three steps: first, the force constants describing the reference surface will be determined from experimental data; second, the structure and force constants of the transition state will be calculated; third, perturbations are applied to the reference surface, perturbed equilibrium- and transition-state structures are calculated, and the former is compared to experiment as is the calculated dependence of activation energy on equilibrium structure.

The necessary force constants are compiled in Table III. The quadratic force constant k_{11} is taken from ab initio calculations on CH_3OCH_3[30] and $CH_3OCH{=}CH_2$[31] after appropriate scaling to reproduce experimental frequencies. The interaction constant k_{12}, or rather the ratio k_{12}/k_{11}, is obtained from ab initio calculations on $HOCH_2OH$.[32,33] Only one of the constants k_{111} and k_{112} can be determined from E_0^* of the reference molecule. The other one is varied within a certain range, producing a corresponding range of transition-state structures (Figure 1, points B–E). A discrimination between these is difficult. However, if we assume that bond distances in transition states follow the same criteria as in ground states, we may require r_1^* and r_2^* to obey the rule of constant bond order, which is so successful in correlating ground-state structures.[21,22] The line of constant bond order intersects the line of transition states having proper E_0^* at point C where $r_1^* = 1.409 + 0.537 \approx 1.95$ Å and $r_2^* = 1.422 - 0.153 \approx 1.27$ Å (Figure 1). The stretching force constant k_{22}^* at this value of r_2^* is 10.8 mdyn Å^{-1}; this is close to estimates from Badger's rule[34] or Herschbach and Laurie's relationship[35] (9.5 mdyn Å^{-1}). It provides additional support for the above assignment of the transition-state structure to point C.[36] The resulting cubic force constants are given in Table III together with some properties of the transition state. An energy contour diagram is given in Figure 4.

The perturbations of the reference surface are represented by a linear term $p(\Delta r_1 - \Delta r_2)$ to be added to the energy expression. The difference $(\Delta r_1 - \Delta r_2)$ accounts for the fact that a change

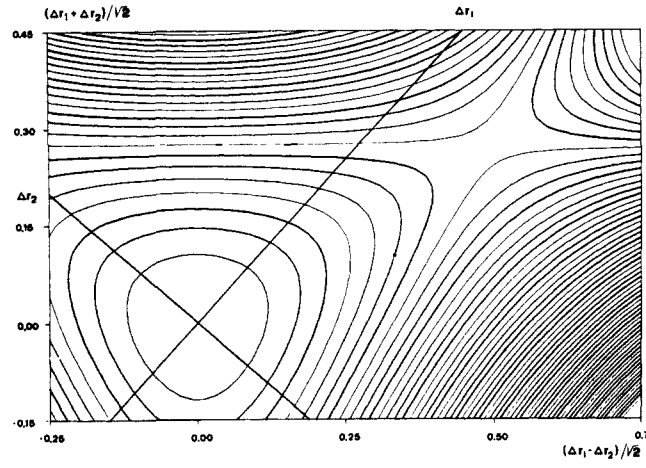

Figure 4. Energy contour diagram for spontaneous acetal cleavage. Ground and transition states are shown. $\Delta r_1 = r_1$ (O1–C1) - 1.409 Å, $\Delta r_2 = r_2$ (C1–O5) - 1.422 Å.

of the exocyclic substituent of **1** affects r_1 and r_2 in opposite directions. The minima and transition states are displaced from their unperturbed values as in the one-dimensional model; the displacements follow, very closely, the curve of constant bond order (Figure 1) and the experimentally observed changes in ground-state structures (Figure 1, stars). Finally, the displacements q_E along the reaction path are calculated from the perturbed values Δr_E and plotted against the perturbed activation energies E^*. The resulting curve is somewhat closer to the experimental data than that obtained with the simple one-dimensional cubic polynomial shown in Figure 2 (dotted line).

Anomeric Effect. As discussed by Jones and Kirby, acetal cleavage occurs readily only if assisted by an anomeric effect between the axial lone pair on O5 and the empty σ^*(C–O) orbital associated with the bond O1–C1. The effect increases in magnitude if the energy gap between the lone pair and σ^*(C–O) orbitals decreases. There is a dynamic and a static mechanism to achieve such an increase.[37]

Consider an asymmetric stretching vibration of the O1–C1–O5 fragment with shortening of r_2 and lengthening of r_1. In the process σ^*(C1–O1) will be lowered and anomeric stabilization increased. This is reflected in the positive sign of k_{12}, which attenuates the cost in stretching energy for an asymmetric motion as compared to a symmetric one. The value of the ratio k_{12}/k_{11} for $HOCH_2OH$ ($\approx$0.05) is significantly larger than corresponding ratios for CH_3OCH_3 (0.009)[30] or $CH_3OCH{=}CH_2$ (0.006)[31] where the anomeric effect between lone pair and σ^*(C–H) is much smaller. The positive value of k_{112} (Table III) has a similar effect. It ensures that the transition state is at $\Delta r_1^* \gg 0$ and $\Delta r_2^* < 0$ (or vice versa). k_{12} and k_{112} may thus be considered to be the origin of the kinetic anomeric effect.[39] In passing we note that the model potential is unrealistic along the line $\Delta r_1 = \Delta r_2$, because it produces another transition state at $\Delta r_1 = \Delta r_2 < 0$.

From a static point of view, consider substitution at O1 by more and more electron-withdrawing substituents. This also lowers the σ^*(C–O) orbital energy, leading to an improved anomeric stabilization, an increased bond order C1–O5 with corresponding bond shortening, and a decreased bond order C1–O1 with corresponding bond lengthening, as observed.[2-4] Thus, structural data and features of the potential energy surface are consistently explained in terms of the same anomeric model.

Ground-State Structures. The observed ground-state structures show that r_1 increases faster than r_2 decreases (Figure 1, stars). This kind of behavior is known for many systems of type X–Y–

(29) This simplifies the expression for E, especially if expressed in terms of symmetry displacement coordinates, $\Sigma = (\Delta r_1 + \Delta r_2)/\sqrt{2}$ and $\Delta = (\Delta r_1 - \Delta r_2)\sqrt{2}$, as $E = k_{\Sigma\Sigma}\Sigma^2/2 + k_{\Delta\Delta}\Delta^2/2 + k_{\Sigma\Sigma\Sigma}\Sigma^3 + k_{\Sigma\Delta\Delta}\Sigma\Delta^2$. The latter expression is simpler to use in numerical calculations.

(30) Blom, C. E.; Altona, C.; Oskam, A. *Mol. Phys.* **1977**, *34*, 557–571 (basis set 4-31G).

(31) Pyckhout, W.; Van Nuffel, P.; Van Alsenoy, C.; Van den Enden, L.; Geise, H. J. *J. Mol. Struct.* **1983**, *102*, 333–345 (basis set 4-21G).

(32) Lehn, J.-M.; Wipff, G.; Bürgi, H.-B. *Helv. Chim. Acta* **1974**, *57*, 493–496 (basis set 3-21G).

(33) Since the factors for scaling diagonal and off-diagonal ab initio force constants are very similar,[30] the ratio k_{12}/k_{11} should be quite reliable and largely independent of basis set deficiencies.

(34) Badger, R. M. *J. Chem. Phys.* **1934**, *2*, 128–131.

(35) Herschbach, D. R.; Laurie, V. W. *J. Chem. Phys.* **1961**, *35*, 458–463.

(36) For $r_i = r_{i0} - 0.20 \log n_i$ we obtain $r_1^* = 1.95$ Å, $r_2^* = 1.29$ Å, and $k_2^* = 8.1$ mdyn Å^{-1}, the latter in even better agreement with estimated values of 8.5 mdyn Å^{-1}.

(37) A quantum chemical justification for such an interpretation follows from the theory of vibronic couplings as summarized by, e.g., Bersuker[25] or Pearson.[38]

(38) Pearson, R. G. *Symmetry Rules for Chemical Reactions*; Wiley-Interscience: New York, 1976.

(39) See, for example: Kirby, A. J. *The Anomeric Effect and Related Stereoelectronic Effects at Oxygen*; Springer-Verlag: Berlin, 1983; p 78 ff.

X[21,22] and has been expressed quantitatively in terms of conservation of bond order. In choosing the functional form of the model potential we do not explicitly invoke any such relationship,[40] yet it is displayed in the behavior of perturbed equilibrium distances (Figure 1, filled circles). This provides additional support for the model, in particular for the anharmonic constants k_{111} and k_{112}.

Transition-State Structures. Transition states derived from both the one-dimensional and the two-dimensional model are closely similar. They are at a distance $q_{TS} \approx 0.55$ Å from the ground state with $r_1^{\ddagger} \approx 1.95$ Å, $r_2^{\ddagger} \approx 1.27$ Å, and a reasonable force constant $k_2^{\ddagger} \approx 10.8$ mdyn Å^{-1}. The exact values depend on the value of the ground-state force constant k_q along the reaction path but are not too sensitive since q_{TS} is proportional to $k_q^{-1/2}$ ($q_{TS} = (6E_0^{\ddagger}/k_q)^{1/2}$). Even a one-dimensional model in combination with the rule of constant bond order provides a reasonable estimate of the transition-state structure.

Our treatment has completely neglected the role of the aqueous solvent. Its potential influence on the transition-state structure may be gauged from ab initio calculations on the water-catalyzed decomposition reactions of $H_2CO_3 \cdot H_2O$,[41] $CH_2{=}C(OH)_2 \cdot H_2O$,[42] and $H_2C(OH)_2 \cdot H_2O$.[43] These proceed through a six-membered transition state (**12**) in which the water molecule accepts a proton from the C–OH group, which becomes the C=O bond in the carbonyl product. This in turn enables the water molecule to efficiently stabilize the leaving OH^- by proton donation. The calculated C–O bond lengthenings $\Delta r_1^{\ddagger}$ are 0.17, 0.34, and 0.38 Å, respectively; the corresponding shortenings $\Delta r_2^{\ddagger}$ are 0.07, 0.11, and 0.16 Å. The transition state becomes more and more late as the "acidity" of the diol reactant decreases. For acetal decomposition there is no proton available on the reactant for donation to a water molecule, and hence the propensity of the latter to stabilize the developing anionic leaving group RO^- by proton transfer is relatively low. The cleavage of the C–OR bond will thus have to advance further before RO^- becomes sufficiently "basic" to interact significantly with solvent water. This qualitative argument is in agreement with a lengthening $\Delta r_1^{\ddagger}$ (0.55 Å) that is larger than that in the various diols. The predicted shortening $\Delta r_2^{\ddagger}$ of 0.15 Å for acetal hydrolysis is somewhat less than that for the methanediol reaction. This is plausible, however, since in the former the $-C{=}O^+-$ distance in the reaction intermediate is 1.25 Å, whereas in the latter the C=O distance in the formaldehyde product is 1.21 Å.[44] Overall, the ab initio calculations on the hydrolysis of $XC(OH)_2$ indicate that for acetal hydrolysis $\Delta r_1^{\ddagger} > 0.38$ Å.

An upper boundary for $\Delta r_1^{\ddagger}$ can be derived from qualitative consideration of the first electronically excited state of the acetal fragment. Promotion of a lone-pair electron from an oxygen into the σ^*(C–O) orbital associated with the other oxygen (Figure 5) leads to a configuration that is repulsive at the ground-state geometry. This configuration correlates with that describing the heterolytically cleaved C–O bond, whereas the electronic ground configuration of the acetal correlates with one corresponding to a homolytically cleaved C–O bond.[45] Configuration interaction between the two states prevents crossing of the two potential curves; it produces a transition state on the ground-state reaction profile and a minimum on the excited-state profile, both at the same geometry[46] (Figure 5). The excited state is characterized by a two-center three-electron C–O bond with electronic configuration $\sigma^2\sigma^{*1}$. In the absence of a half-occupied lone-pair orbital

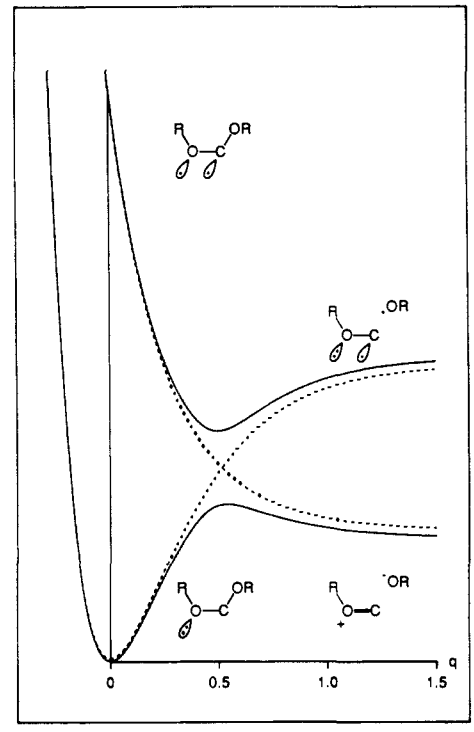

Figure 5. Schematic representation of the energy of the electronic ground and first excited states (lp → σ^*) as a function of q.

the equilibrium distance of such a bond may be estimated to be 2.2 Å. The estimate is based on an ab initio distance of 2.16 Å for $(H_3N{\div}NH_3)^+$[47] and on crystal structure analysis of **13** and **14** with distances of 2.30[48] and 2.16[49] Å, respectively. The main effect of configuration interaction in the acetal fragment is to delocalize the σ^* electron into the lone-pair orbital and consequently to dampen its antibonding effect (not possible in the N–N systems). This is consistent with an increase of the C–O distance in the transition state of $\Delta r_1^{\ddagger} < 0.7$ Å, i.e. $r_1^{\ddagger} < 2.2$ Å.

In summary, comparison of the transition-state electronic and geometric structure for spontaneous acetal cleavage with related systems of similar electronic structure imposes a lower limit of 0.4 Å and an upper limit of 0.7 Å on $\Delta r_1^{\ddagger}$ ($1.8 < r_1^{\ddagger} < 2.2$ Å). Both limits are compatible with the transition-state C–O distances derived from our simple model ($r_1^{\ddagger} \approx 1.94$ Å).

Structure–Reactivity Correlations versus Reaction Profile. Structure–reactivity correlations are expressed quantitatively in terms of the dependence of $E^{\ddagger}$ on q_E (Figures 2 and 3). The calculated correlations are closely similar in the one- and two-dimensional models. Thus even the simple one-dimensional model yields an excellent approximation to the observed structure–reactivity relationship. It remains to be seen whether further refinement of the model, including changes in bond angles and torsion angles, improves the agreement.

Jones and Kirby[4] represented their data in terms of a structure–reactivity correlation ($E^{\ddagger}$ versus r_1), which was interpreted as mapping out "a curve parallel to the reaction coordinate for the cleavage of the parent acetal" and defining "the slope of the reaction coordinate in this region".[4] Figure 3 demonstrates the relationship between a structure–reactivity correlation, on the one hand, and the reaction profile for an individual molecule, on the other. The dotted line, which represents the $E^{\ddagger}$–q_E correlation ($E^{\ddagger}$ versus r_1 in ref 4) is seen to be quite different from the potential energy function of either the unperturbed or a perturbed molecule. Extrapolation of the structure–reactivity correlation leads to $\Delta r_1^{\ddagger} \approx 0.15$ Å ($r_1^{\ddagger} = 1.56$ a, Figures 3–5 in ref 4), much

(40) Although it is invoked in fixing a *numerical* parameter.
(41) Nguyen, M. T.; Hegarty, A. F.; Ha, T.-K. *THEOCHEM* **1987**, *150*, 319–325 (basis set 3-21G).
(42) Nguyen, M. T.; Hegarty, A. F. *J. Am. Chem. Soc.* **1984**, *106*, 1552–1557 (basis set STO-3G).
(43) Williams, I. H.; Spangler, D.; Femec, D. A.; Maggiora, G. M.; Schowen, R. L. *J. Am. Chem. Soc.* **1983**, *105*, 31–40 (basis set STO-3G).
(44) It is interesting to note that the calculated transition-state distances $r_1^{\ddagger}$ and $r_2^{\ddagger}$ for $CH_2(OH)_2 \cdot H_2O$ follow the rule of constant bond order, $r_i - r_{i_0} = c \ln n_i$. Here c (0.306 Å) is obtained from the C–OH and C=O distances (1.429 and 1.217 Å).[43]
(45) Shaik, S. S. *J. Am. Chem. Soc.* **1981**, *103*, 3692–3701.
(46) Bersuker, I. B.; Gorinchoi, N. N.; Polinger, V. Z. *Theor. Chim. Acta* **1984**, *66*, 161–172.
(47) Bouma, W. J.; Radom, L. *J. Am. Chem. Soc.* **1985**, *107*, 345–348 (basis set 6-31G*).
(48) Alder, R. W.; Orpen, A. G.; White, J. M. *J. Chem. Soc., Chem. Commun.* **1985**, 949–951.
(49) Gerson, F.; Knöbel, J.; Buser, U.; Vogel, E.; Zehnder, M. *J. Am. Chem. Soc.* **1986**, *108*, 3781–3783.

too small for the reaction to be described as proceeding through a late transition state.[5] The transition-state structures calculated from reaction profiles are more in line with mechanistic and kinetic information. Finally, we note that an $E^{\ddagger}$ versus q_E correlation allows an estimation of force constants, or, conversely and probably more important, a knowledge of quadratic force constants can yield a prediction of the dependence of reaction rate on structure.

Reaction Path versus Response Path. Given an energy surface, a reaction path may be traced by starting at the transition state, proceeding along the direction of maximum negative curvature (reaction coordinate), and following the direction of steepest descent to the ground state. When this procedure is applied to the energy surface in Figure 4, a straight line is obtained (connecting point C with the origin in Figure 1). This line may be compared to the curve derived from the mapping procedure on the basis of perturbed ground-state structures (Figure 1, stars and filled circles). The reaction path for a specific molecule is close to but not quite identical with the "reaction path" derived from the mapping procedure. The latter is a reponse path[50] reflecting the energy surface of the reference molecule as well as the direction and magnitude of the perturbations needed to model the effects of varying leaving groups.

Energy and Structure Correlation. The comparison of the sequence of ground-state structures (Figure 1, filled circles and stars) with the reaction path for a specific molecule bears on a basic assumption behind the structure correlation method, namely that "a distribution of sample points corresponding to observed structures will tend to be concentrated in low-lying regions of the potential energy surface" and that "the interaction energy between the molecule or molecular fragment of interest and its various crystal or molecular environments can be regarded as a small perturbation relative to the total molecular potential energy".[50] Both statements are borne out by the treatment presented here.

Conclusion and Outlook. We have shown that changes in ground-state structure and changes in reaction rate constants can be correlated in terms of simple models involving energy surfaces parametrized with the help of structural, vibrational, electronic, kinetic, and mechanistic information on reactants. The models give estimates of transition-state structure, which are consistent with a variety of evidence: simple extrapolations based on the principle of structural correlation,[20,21,50] qualitative arguments about the electronic structures of reactants, products and transition states, and a large body of qualitative mechanistic information. Extension to more elaborate models (e.g. higher order expansions of E or inclusion of more geometrical parameters) is possible provided the necessary additional information is available, e.g. structures, force constants, electronic spectra, equilibrium constants, reactants, kinetic isotope effects, product ratios, free energy relationships, mechanistic information on the role of catalysts, etc. In this sense, the approach is quite general. Although it uses a number of concepts that have been described before,[3] we are not aware of a treatment that simultaneously incorporates the same diversity of observable quantities into a single model and that provides a comparable range of detailed information on the reactivity and transition-state structures for a series of related molecules.

The differences between reactions of different substrates are often discussed in terms of relative ground- and transition-state stabilization or destabilization. There is a problem, however; experimentally we obtain free energies of activation, which are differences between the ground- and transition-state energies. Differences between free energies of activation are therefore differences between differences. Associating such second differences with either the ground or the transition state is arbitrary unless an absolute reference energy for a series of different (albeit related) molecular systems can be defined. If we consider the perturbing forces instead, the perturbation of ground- and transition-state structures may be estimated by approximating the energy profile at either structure as a quadratic potential $E = k_E(q - q_E)^2/2$ and $E = k_{TS}(q - q_{TS})^2/2$, respectively. Upon perturbation ($a_E q$ or $a_{TS} q$) q_E changes to $q_E + a_E/k_E$ and q_{TS} to $q_{TS} + a_{TS}/k_{TS}$. The changes are seen to depend on the ratio of a and k but not on an arbitrary allocation of the change in activation energy to one of the two states. Depending on the sign and magnitude of a_E/k_E and a_{TS}/k_{TS}, the perturbed sytem can be said to be primarily ground-state stabilized ($-\Delta q_{TS} < \Delta q_E > 0$), transition-state stabilized ($-\Delta q_E < \Delta q_{TS} < 0$), or destabilized ($\Delta q_E < 0$ and $\Delta q_{TS} > 0$). In the example discussed above the linearly perturbed cubic polynomial leads to $\Delta q_E = -\Delta q_{TS}$; i.e., both states are equally affected. Another example is metallacyclopentene ring inversion in s-*cis*-η^4-butadiene metallocene complexes (**15a** — **15b**);[2] it is

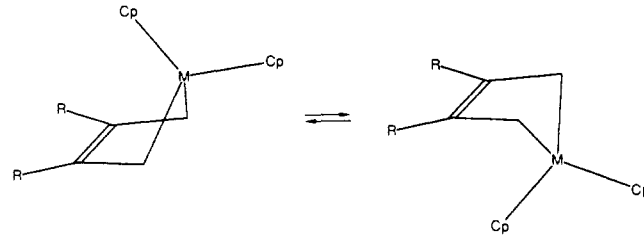

(15a) (15b)

energetically degenerate. For symmetry reasons the transition-state structure is characterized by a planar metallacyclopentene ring. The reaction profile was modeled by a symmetric quartic polynomial and perturbed by a symmetric quadratic function. This leads to $\Delta q_E \neq \Delta q_{TS} = 0$ and corresponds to ground-state (de)stabilization. In the case of an exponentially perturbed Morse potential ($n < 1$), $\Delta q_E > 0$ and $\Delta q_{TS} = 0$ (q_{TS} is at infinity). This agrees with the common chemical notion that the bond energy of long bonds (e.g. single bonds) is smaller than that of short bonds (e.g. double bonds). This phraseology is similar to Thornton's "force formulation"[1] but avoids the "perpendicular effects" (displacement of the reaction profile along the energy coordinate).[3]

The phenomenon of selectivity may be discussed along similar lines. Recently, Seebach et al.[51] have shown that the sp^2-hybridized carbons in 2,6-disubstituted 1,3-dioxin-4-ones with sofa-type conformation are slightly pyramidalized (**16**). Addition of

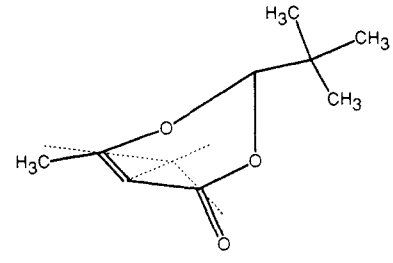

(16)

cuprates to and reduction by H_2 (Pd/C) of these centers occur stereospecifically from the (sterically more hindered) side to which the pyramid points. Both the ground-state deformation and the direction of attack are traced to the same cause, namely a tendency to minimize torsional strain in both the ground and the transition state. Attack from the sterically less hindered side would have to overcome ground-state pyramidalization and would increase torsional strain on the way to the transition state. In terms of the cubic model outlined above, the former situation corresponds to perturbation of the reaction profile for a (hypothetical) planar reference structure by a curve with negative slope ($a < 0$), leading to a decrease in activation energy, and the latter to a perturbation with positive slope ($a > 0$), leading to an increase in activation energy.

It has been argued that the role of an (enzymatic) catalyst is to bind and immobilize a substrate in a reactive conformation showing optimal steric and stereoelectronic features, to strain the substrate, structurally and electronically, toward a transition state,

(50) Bürgi, H. B.; Dunitz, J. D. *Acc. Chem. Res.* **1983**, *16*, 153–161.

(51) Seebach, D.; Zimmermann, J.; Gysel, U.; Ziegler, R.; Ha, T.-K. *J. Am. Chem. Soc.* **1988**, *110*, 4763–4772.

and to stabilize the latter.[3,52] In view of the above discussion these functions may be interpreted as different aspects of the same cause, namely a structural and electronic perturbation of the substrate by the enzyme everywhere along the reaction profile. In the ground state small but specific structural and electronic changes in the bonded substrate are induced, the associated cost in enthalpy and entropy being modest and/or overcompensated by binding energy. The perturbation changes dramatically on going to the transition state. Resulting rates of change may amount to as much as 10 kcal in free energy of activation per 0.05 Å of ground-state structural change (Figure 3), corresponding to an acceleration of 10^7 at room temperature. The structural changes necessary for significant changes in rate may be compared, for example, with the observed variation of C=O and C-N equilibrium distances in amides. They depend on the degree of protonation and vary from 1.24 and 1.35 Å for a standard amide group in a helix or pleated sheet structure to 1.28 and 1.30 Å, respectively, in a hemiprotonated amide group (RHN-RCO···H···OCR-NHR).[52] Thus, even partial protonation induces structural changes large enough to account for significant changes in reactivity.

For many reactions, especially organic ones, the differences in ground-state structures may be quite small, whereas the associated rate differences may be relatively large. This points to a need for accurate structure determinations for a series of molecules, preferably in conjunction with corresponding kinetic and mechanistic experiments. Significant structural differences indicating incipient reaction toward the transition state and corresponding kinetic differences are likely to be found whenever a steric or electronic difference between related reactants can be identified. In these cases ground-state structure is related to reactivity in a quantitative and predictable way.

Acknowledgment. We thank Professors Bersuker, Dunitz, and Kirby for their comments and the Schweizerischer Nationalfonds zur Förderung der wissenschaftlichen Forschung for financial support.

Supplementary Material Available: Tables of scaled internal coordinates and inertial coordinates and a figure with results of principal component analysis (5 pages). Ordering information is given on any current masthead page.

(52) For a review, see: Gorenstein, D. G. *Chem. Rev.* **1987**, *87*, 1047-1077.
(53) Dunitz, J. D.; Winkler, F. K. *Acta Crystallogr., Sect. B: Struct. Crystallogr. Cryst. Chem.* **1975**, *B31*, 251-263.

S-S Bond Lengths, or Can a Bond Length Be Estimated from a Single Parameter?

Osvald Knop, Russell J. Boyd,* and S. C. Choi

Contribution from the Department of Chemistry, Dalhousie University, Halifax, Nova Scotia, B3H 4J3 Canada. *Received February 5, 1988*

Abstract: The results of 6-31G* optimizations of the equilibrium molecular geometries of S_2^ϵ ($-2 \le \epsilon \le +2$), $X(SS)_2^\epsilon$ (C_2; X = P, S, Cl; $-3 \le \epsilon \le -1$), $SO_{4-n}S_n^{2-}$ (n = 1-4), S_2O, X_2S_2 (C_2; X = H, F, Cl), and SSF_2 are reported in detail and compared with experiment. The calculated bond lengths r_e(S-S) in these molecular species exhibit a high degree of correlation (r^2 = 0.97) with the electron densities $\rho(\mathbf{r}_c)$ at the critical points in these bonds, $r_e(S-S) = 1.229[\rho(\mathbf{r}_c)]^{-0.269}$. This power-law relationship, the analogue of which has been demonstrated for Al-F, O-O, and Be-Cl bonds and which is expected to be of general validity, makes possible estimates of r_e from $\rho(\mathbf{r}_c)$ and, conversely, estimates of $\rho(\mathbf{r}_c)$, bond order, and related properties from r_e.

The answer to the title question appears to be a cautious yes. The parameter is the electron density $\rho(\mathbf{r}_c)$ at the bond critical point, i.e., at the point where the density is a minimum with respect to a displacement along the bond path but a maximum with respect to a lateral displacement ($\nabla\rho(\mathbf{r}_c) = 0$).[1,2] In the following we demonstrate the existence of a simple correlation between the bond length r_e and $\rho(\mathbf{r}_c)$ for S-S bonds, both obtained from 6-31G* optimizations[3-5] of the equilibrium geometries of a number of simple molecular species. While the present demonstration involves *calculated* r_e (Å) and $\rho(\mathbf{r}_c)$ (au), we have no reason to suppose that it would not apply equally to experimental r_e,$\rho(\mathbf{r}_c)$ pairs. Since $\rho(\mathbf{r}_c)$ is accessible to experiment with difficulty, the practical value of the correlation may well be in its reverse, i.e., using the bond length to estimate $\rho(\mathbf{r}_c)$ and in turn quantities related to it, e.g., the bond order[2] or, in a more restrictive context, the force constants of S-S bonds.[6] However, the main point we wish to make is that the existence of such a correlation within a given optimization scheme is by itself of interest, regardless of the merits or demerits of our particular 6-31G* basis set in relation to experiment or to other theoretical treatments.

Table I. Optimized Equilibrium Molecular Parameters (6-31G*) of S_2^ϵ Species

No.	species	$E_{6\text{-}31G^*}$, au	$\rho(\mathbf{r}_c)$, au	S-S, Å	
				calcd	obsd
1	S_2 ($X^3\Sigma_g^-$)	-795.016 58	0.205 47	1.8782	1.8894[8]
2	S_2 ($a^1\Delta_g$)	-794.964 06	0.205 59	1.8779	1.8983[9]
3	S_2^+ ($X^2\Pi_g$)	-794.669 06	0.243 79	1.7879	1.8240 (2)[10]
4	S_2^{2+}	-794.046 21	0.275 79	1.7196	
5	S_2^-	-795.046 26	0.160 46	2.0000	
6	S_2^{2-}	-794.847 48	0.104 81	2.2020	*a*

[a] The values observed in crystals range from ~2.03 to ~2.36 Å. They depend strongly on the nature of the countercation and on the physical properties of the crystal. The two values included in the inset of Figure 1 are those for the two much studied forms of FeS_2, pyrite, and marcasite (unlabeled).

The r_e vs. $\rho(\mathbf{r}_c)$ correlation for S-S bonds is based on an extension of our 6-31G* treatment of isoelectronic XL_4^ϵ species.[7]

(1) Bader, R. F. W. *Acc. Chem. Res.* **1985**, *18*, 9.
(2) Bader, R. F. W.; Tang, T.-H.; Tal, Y.; Biegler-Kõnig, F. W. *J. Am. Chem. Soc.* **1982**, *104*, 946.
(3) Binkley, J. S.; Whiteside, R. A.; Krishnan, R.; Seeger, R.; Defrees, D. J.; Schlegel, H. B.; Topiol, S.; Kahn, L. R.; Pople, J. A. GAUSSIAN 80, Department of Chemistry, Carnegie-Mellon University, Pittsburgh, PA, 1983.
(4) Frisch, M. J.; Binkley, J. S.; Schlegel, H. B.; Raghavachari, K.; Melius, C. F.; Martin, R. L.; Stewart, J. J. P.; Bobrowicz, F. W.; Rohlfing, C. M.; Kahn, L. R.; Defrees, D. J.; Seeger, R.; Whiteside, R. A.; Fox, D. J.; Fleuder, E. M.; Pople, J. A. GAUSSIAN 86, Carnegie-Mellon Quantum Chemistry Publishing Unit, Pittsburgh, PA, 1984.
(5) Bader, R. F. W. AIMPAC series of programs, Department of Chemistry, McMaster University, Hamilton, Ont., Canada, 1983.
(6) Steudel, R. *Z. Naturforsch., B* **1975**, *30*, 281.
(7) Choi, S. C.; Boyd, R. J.; Knop, O. *Can. J. Chem.* **1987**, *65*, 1109.

0002-7863/88/1510-7299$01.50/0